Desalination and Water Treatment
www.deswater.com

doi: 10.1080/19443994.2014.985721

57 (2016) 3283–3291
February

Taylor & Francis
Taylor & Francis Group

Cadmium removal from aqueous solution using nano/milli-sized particles of cedar leaf ash

Laleh Divband Hafshejani[a,*], Saeed Boroomand Nasab[a], Mostafa Moradzadeh[a], Sara Divband[b], Jahangir Abedi Koupai[c]

[a]*Faculty of Water Sciences Engineering, Department of Irrigation and Drainage Engineering, Shahid Chamran University of Ahvaz, Ahvaz, Khuzestan, Iran, Tel. +98 9132387133; Fax: +98 6133330635; emails: mdivband@gmail.com (L. Divband Hafshejani), boroomandsaeed@yahoo.com (S. Boroomand Nasab), moradzadeh.mostafa@gmail.com (M. Moradzadeh)*
[b]*Faculty of Natural Resources, Agricultural Sciences and Natural Resources University of Gorgan, Golestan, Iran, email: saradivband@yahoo.com*
[c]*Department of Water Engineering, College of Agriculture, Isfahan University of Technology, Isfahan, Iran, email: koupai@cc.iut.ac.ir (J. Abedi Koupai)*

Received 16 February 2014; Accepted 24 October 2014

ABSTRACT

Heavy metals in water resources are one of the important environmental problems. These metals have hazardous effects on human health. This study was conducted to investigate the comparison between adsorption of cadmium from aqueous solution using nano/milli-sized adsorbents of cedar leaf ash by batch experiments and with variation of impressive parameters such as pH, contact time, and adsorbent amount. The results showed, the optimum pH of adsorption was 5. Adsorption equilibrium times for nano/milli-sized adsorbents were obtained in 30 and 45 min, respectively. With increasing the amount of milli-sized adsorbent, adsorption efficiency increased but increasing of nanosized adsorbent at first, caused the increase in adsorption efficiency and then adsorption efficiency decreased because of clogging phenomenon of adsorbent in aqueous solution. The experimental data were analyzed using two isotherm models (Langmuir and Freundlich) and two kinetic models (pseudo-first-order and pseudo-second-order). Based on the results, adsorption of cadmium followed from the models of pseudo-second-order kinetic and Langmuir isotherm well. Adsorption capacity of nanosized adsorbent was about two times more than adsorption capacity of milli-sized adsorbent. This case indicated the high ability of nanoparticles in adsorption of cadmium from aqueous solution.

Keywords: Cadmium; Adsorption; Cedar leaf ash; Nanoparticles

1. Introduction

Toxic heavy metals pollution is one of the influential environmental problems, because they are nondegradable and harmful for public health, even at very low concentrations [1]. One of the most pollutant heavy metals is cadmium, which is extensively used in industrial processes. Cadmium removal from water and wastewater has become a main environmental matter due to its hazardous effects on human health [2–5]. The US Environmental Protection

---

*Corresponding author.

Agency has set new stringent standards for cadmium, at 5.00 μg L^{-1} [6]. Various methods were applied to remove heavy metals from waters and wastewaters including ion exchange, adsorption, precipitation, coagulation/flocculation, membrane filtration, and electrolysis [6–10]. These methods have some disadvantages, for example, high cost, time-consuming, and secondary waste [11]. The use of nanotechnology is one of the fundamental methods to solve the shortcomings of mentioned methods [10].

Nanoparticles due to their unique specifications such as small size, large surface area, crystal shape, and high reactivity are used for refining pollutants from aqueous solution [12]. In recent years, the application of agricultural wastes as low-cost adsorbents has attracted attention of many researchers [8,13–15]. These materials consist mainly of lignin and cellulose [16].

Cedar with scientific name of Zizyphus spina christi grows in Saudi Arabia, north of Africa, and in Iran in provinces of Khuzestan, Fars, and Hormozgan.

In the present study, a series of batch experiments were performed to assess the ability of nano/milli-sized particles prepared from the cedar leaf ash for cadmium removal. Effects of various parameters were examined, such as pH, contact time, and adsorbent amount, on the adsorption of cadmium. Finally, adsorption processes were evaluated with kinetic and isotherm models and the best models were defined.

2. Materials and methods

This research was conducted in lab scale via batch experiments. Soluble metals with a volume of 100 mL at a concentration of 10 mg L^{-1} was prepared from cadmium chloride. HCl and NaOH were used to adjust the pH values. All the experiments were conducted at a constant temperature of 20 ± 2˚C.

2.1. Preparation of adsorbent

Cedar leaves after washing were dried at temperature of 105˚C for 1 h, and then the leaves were carbonized by muffle furnace at 600˚C for 40 min to obtain the ash. For preparing adsorbent with millimeter size, leaves ash were crushed by mortar. For preparing adsorbent in nanometer scale, the crushed ash was spilt to ball mill (D-56070 KOBLENZ model, Germany). Then stearic acid (material process controller) was added to adsorbent with amount of 2% of the adsorbent weight. Particle size analyzer (PSA, Malvern Zetasizer 3000, and UK) was used to characterize the particles size of nanosized adsorbent. For millimeter particle size, the adsorbent grading between two sieve numbers of 18 and 20 (0.841–1 mm) were used. The specific surface area of the adsorbents was characterized by the method of methylene blue [17–19]. Elemental (C, H, N, S, and O) analyses were conducted using a CHNSO analyzer (vario ELIII-elementar, Germany). Morphology of adsorbent surfaces was determined by scanning electron microscopy (SEM, Leo 1455 VP model, Germany) [2]. Fourier transform infrared spectroscopy (FTIR) spectra were obtained with a FTIR (Spectrum GX, Perkin-Elmer).

2.2. Determination of optimum pH

Determination of optimum pH was performed by mixing 1 g adsorbent with a 100 ml cadmium solution at a concentration of 10 mg L^{-1}. The pH value of solutions was adjusted between 3 and 8. Then, they were shaken in controlled temperature for 12 h with a speed of 150 rpm. For determination of the adsorbent pH_{pzc}, 100 mL 0.01 M NaCl solution was spilt into several closed Erlenmeyer flasks. The initial pH of solutions was adjusted between 3 and 8 by adding 0.1 M HCl or 0.1 M NaOH. Then 1 g adsorbent was added to each solution, the mixtures were shaken in controlled temperature for 48 h with a speed of 150 rpm. The final pH was measured after 48 h [20,21].

2.3. Kinetic adsorption experiments

A kinetic study was performed to examine the rate-controlling mechanism of the adsorption of cadmium ions by prepared adsorbents [22]. One gram of adsorbent was added to 100 mL solution containing cadmium ions with an initial concentration of 10 mg L^{-1}. These solutions were shaken at time of 5, 10, 15, 30, 45, 60, 90, and 120 min and with a speed of 150 rpm [23]. After that, liquid and solid phases were separated and the concentration of cadmium was determined by atomic adsorption spectrometry (Varian 220 FS AA model). Pseudo-first-order and pseudo-second-order kinetic models were used to illustrate the experimental data.

2.4. Adsorption isotherm experiments

The equilibrium adsorption isotherms are one of the most important approaches to understand the procedure of adsorption [24]. Batch isotherm studies were conducted by varying mass of adsorbate. One gram of nano/milli-sized adsorbents were mixed with 100 mL of solutions containing cadmium ions at the concentration range of 2, 10, 25, 40, and 50 mg L^{-1}. The mixtures were shaken at 20˚C with 150 rpm for 30 and 45 min for nano/milli-sized adsorbents, respectively [23,25].

Then Langmuir and Freundlich models were fitted on experimental data. The Freundlich isotherm is appropriate to both monolayer and multilayer adsorption and is based on the assumption that the adsorbates are adsorbed onto the heterogeneous surface of an adsorbent [26]. The Langmuir isotherm assumes monolayer adsorption on a uniform surface with a finite number of adsorption sites [27].

The equations and parameters of kinetics and isotherms of this research have been presented in Tables 1 and 2, respectively.

Root mean square error (RMSE) and coefficient of determination (R^2) were used to evaluate the models of this research.

- Coefficient of determination (R^2)

$$R^2 = \frac{\left(\sum_{i=1}^{N} \left(O_i - \overline{O}\right)\left(P_i - \overline{P}\right)\right)^2}{\sum_{i=1}^{N} \left(O_i - \overline{O}\right)^2 \cdot \sum_{i=1}^{N} \left(P_i - \overline{P}\right)^2} \tag{1}$$

The values of R^2 ranges from 0.0 to 1.0, indicating a better agreement for the values close to 1.0.

- RMSE

$$\text{RMSE} = \sqrt{\frac{1}{n-2} \sum_{i=1}^{n} (O_i - P_i)^2} \tag{2}$$

The RMSE has minimum value of 0.0, with a better agreement close to 0 [31]. Here n, number of observations; O_i, ith value of the observed measurement; P_i, ith value of the predicted measurement; $\bar{O}$, mean of the observed values; and $\overline{P}$, mean of the predicted values.

3. Results and discussion

3.1. Adsorbents properties

Figs. 1 and 2 show the SEM images of adsorbents. These figures show pores with different sizes on the adsorbent surface.

Table 1
Equation model used in this study

Nonlinear equation	Model
$q_t = q_e[1 - \exp(-K_1 t)]$	Pseudo-first-order (Kinetic) [28]
$q_t = \dfrac{K_2 q_e^2 t}{1 + q_e K_2 t}$	Pseudo-second-order (Kinetic) [28]
$q_e = K_f c_e^{\frac{1}{n}}$	Freundlich (isotherm) [28,29]
$q_e = \dfrac{b q_m c_e}{1 + b c_e}$	Langmuir (isotherm) [28,30]

Table 2
Model parameters used in this study

Coefficient	Description
q_e	adsorption capacity at equilibrium (mg g^{-1})
q_t	adsorption capacity at time t (mg g^{-1})
q_m	maximum adsorption capacity (mg g^{-1})
K_1	rate constant of the pseudo-first-order adsorption (min^{-1})
K_2	rate constant of the pseudo-second-order adsorption (g mg^{-1} min)
c_e	concentration of solute in solution at equilibrium time (mg cm^{-3})
n	Freundlich isotherm exponent (dimensionless)
K_f	Freundlich isotherm constant (dimensionless)
b	Langmuir constant (L mg^{-1})

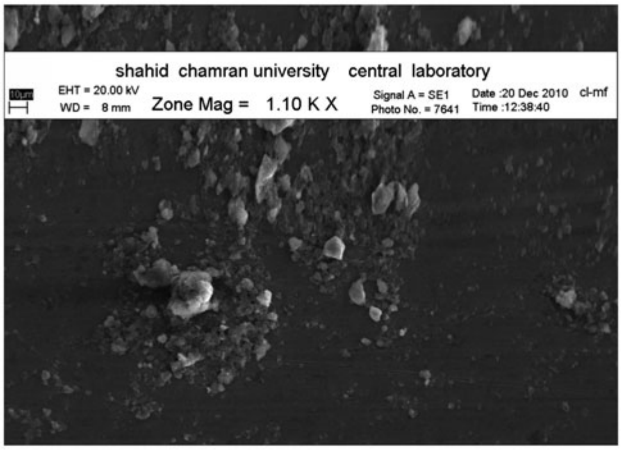

Fig. 1. SEM image of nanosized adsorbent of cedar leaf ash.

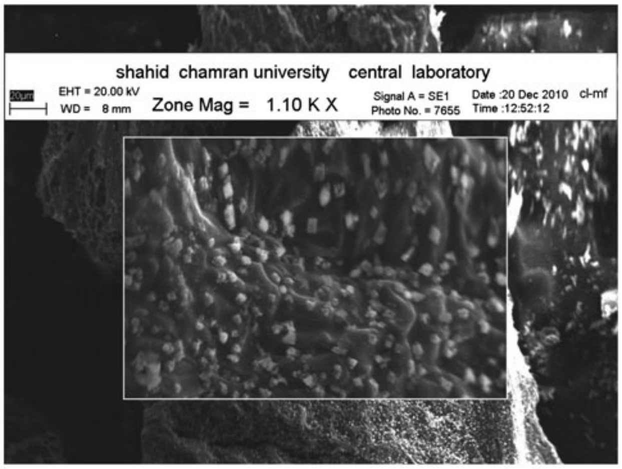

Fig. 2. SEM image of milli-sized adsorbent of cedar leaf ash.

Fig. 1 shows that nanoparticles have a tendency to clog up. It reveals that the agglomeration process significantly causes change in size of the particles and it depends on the amount of adsorbent in the solution [32].

The particles of milli-sized adsorbent of cedar leaf ash were obtained with diameter of 0.841–1 mm (the adsorbent grading between two sieve numbers of 18 and 20). The particles size results of nanosized adsorbent of cedar leaf ash is shown in Fig. 3. The results of particle size analyzer showed that all particles were smaller than 207 nm.

Specific surface area of nano/milli-sized adsorbent of cedar leaf ash was measured 33.53 and 20.38 $m^2 g^{-1}$ respectively by the methylene blue method. The results of elemental (C, H, N, S, and O) analyses are listed in Table 3.

FTIR is often used to characterize functional groups of the adsorbents for heavy metal ions adsorption [3,24]. FTIR spectrum of cedar leaf ash before and after adsorption, in the range of 500–4,000 cm^{-1} is shown in Fig. 4. FTIR spectrum of after adsorption shows wavenumber and the intensity of some peaks is shifted or substantially lower than those before adsorption.

The adsorption band of O–H and N–H groups is shifted from 3,342 to 3,195 cm^{-1} [33–36]. The peak at 1,616 cm^{-1} indicates the presence of C=O or C=C groups [36,37]. The peaks at 1,313 and 1,396 cm^{-1} show the presence of N–H group [33]. The peak at 1,078 cm^{-1} is attributed to C–OH stretching vibration [33,36]. The absorption band appearing at 1,078 cm^{-1} has shifted to 1,124 cm^{-1}. The weak bands at 418 and 516 cm^{-1} in the spectrum show N–H and P–O groups, respectively [33]. After cadmium adsorption, peak at 418 and 516 cm^{-1} has shifted to 470 and 603 cm^{-1}, respectively.

Table 3
Elemental contents of cedar leaf ash (%)

C	57.46
H	4.205
N	2.808
S	0.829
O	34.698

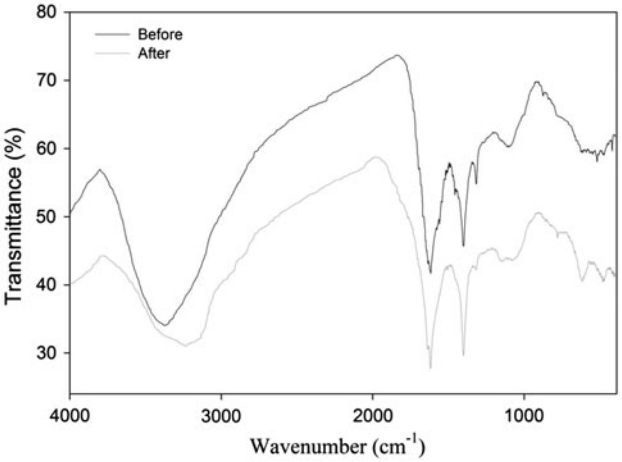

Fig. 4. FTIR spectrum of cedar leaf ash.

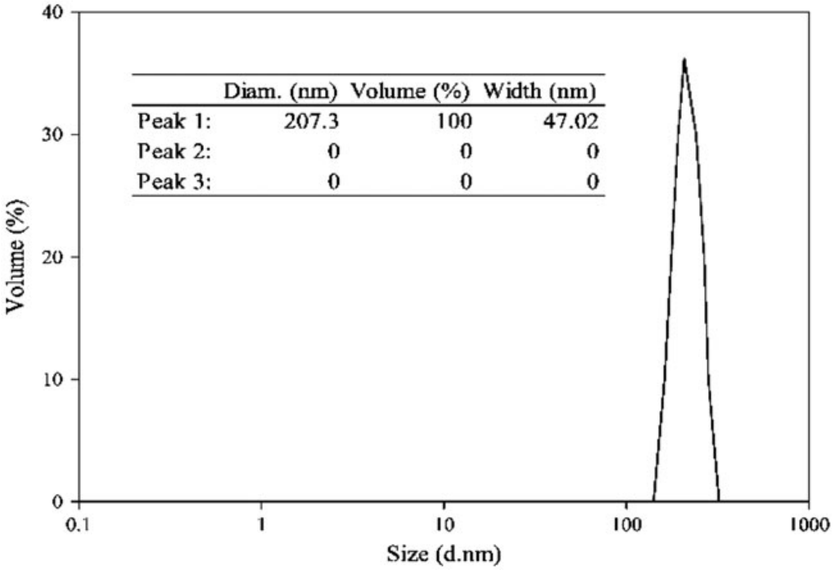

	Diam. (nm)	Volume (%)	Width (nm)
Peak 1:	207.3	100	47.02
Peak 2:	0	0	0
Peak 3:	0	0	0

Fig. 3. The particles size distribution of nanosized adsorbent.

3.2. Effect of pH

One of the most important parameters that effect on adsorption, is pH of solution [5,38]. It seems that at low pH (pH 3) H^+ ions are serious competitor for cadmium ions, so that affected the performance of adsorbents for the adsorption of cadmium. With the increasing pH and decreasing competitor ions, difference between the nano/milli-sized adsorbents of cedar leaf ash performance in absorption of cadmium is determined. At high pH, presence of OH^- ions on the surface of adsorbent provide the higher potential for cadmium adsorption.

The adsorption percentage of cadmium vs. pH variation is shown in Fig. 5.

The minimum and maximum adsorptions occurred at the pH of 3 and 5, respectively. In this research with increase in the pH from 3 to 5, adsorption percentage increases. For experiments of determination of the optimum pH, at first, ranges of pH were 3–8. During the experiments, with increasing pH ($pH > 5$), no adsorption experiments were conducted because white Cd $(OH)_2$ precipitate was formed. Similar behavior has been reported by Huang and Chen [39]. In fact since at pH more than 5, Cd $(OH)_2$ will precipice and some cadmium ions will omit, and according to the main objective of this research which was cadmium elimination only by adsorption mechanism, surveying the amount of adsorption at pH more than 5 by nano–milli structure of cedar leaf ash was not possible. Cadmium ions adsorption efficiency was determined from the following equation [6,9,40]:

$$E_a = \frac{C_0 - C_e}{C_0} \times 100 \tag{3}$$

where E_a is adsorption efficiency, C_0 and C_e are the initial and equilibrium concentrations of cadmium ions in the solution ($mg\,L^{-1}$), respectively.

Considering to resemblance the chemical structures of two adsorbents, difference in their performance is related to particle size of adsorbents. In fact, there is an inverse relationship between the particle size and removed contaminants percentage. Whenever the particle size of adsorbents decreases, the adsorption efficiency increases because of the enlargement of the specific surface area and more availability of metal ions for adsorption locations. The result showed that the pH_{pzc} is equal to 3.76. At the pH higher than the pH_{pzc}, the surface of the adsorbent is negatively charged, favoring the adsorption of cationic species. Also, adsorption of anionic species will be favored at pH lower than the pH_{pzc} [23,24].

3.3. Kinetic study

Fig. 6 shows the adsorption of cadmium vs. time. Results showed for two adsorbents, with increase of contact time, adsorption percentage increases. Maximum percentage of adsorption was obtained after 30 and 45 min for nano/milli-sized adsorbent, respectively. Increase in contact time after mentioned times is not effective in adsorption of cadmium ions. Also, results of other researchers confirm the positive effect of contact time of adsorbent and solution on contamination removal [32,38,41,42].

The kinetic parameters computed from the pseudo-first- and the pseudo-second-order models are listed in Table 4, and the plots of two kinetic models are shown in Figs. 7 and 8.

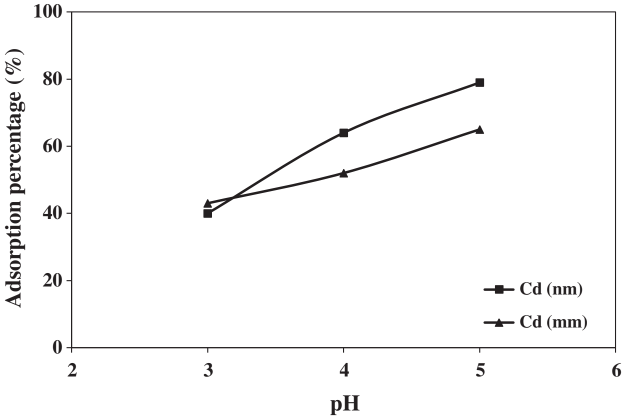

Fig. 5. Effect of pH on adsorption of cadmium (initial concentration of solution, $10\,mg\,L^{-1}$; adsorbent amount, $10\,g\,L^{-1}$).

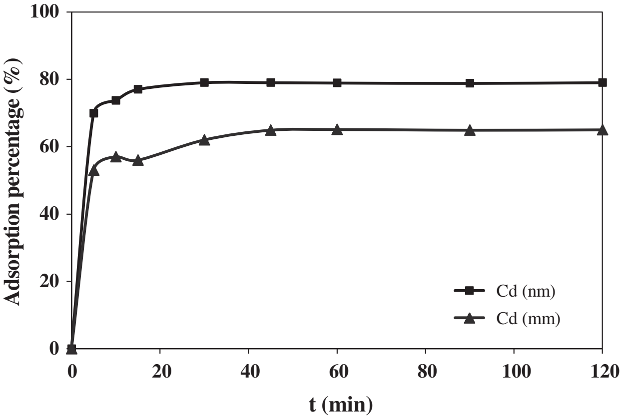

Fig. 6. Effect of contact time on adsorption of cadmium (initial concentration of solution, $10\,mg\,L^{-1}$; adsorbent amount, $10\,g\,L^{-1}$; pH 5).

Considering Table 4 for study of adsorbents, both mentioned models, describe adsorption process well but the pseudo-second-order model for nanosized adsorbent of cedar leaf ash (RMSE = 0.00624 and R^2 = 0.9995) compared with the pseudo-first-order model (RMSE = 0.01531 and R^2 = 0.9969) has a better fitting of experimental data. Also this model has best fitting on adsorption of cadmium by milli-sized adsorbent of cedar leaf ash (RMSE = 0.01223 and R^2 = 0.9981). The results indicate that the rate constant of pseudo-second-order adsorption for nano/milli-sized adsorbents are 1.728 and 1.132, respectively. The rate constant of pseudo-first-order adsorption for nanosized adsorbent compared with milli-sized adsorbent has a greater amount (0.4249–0.3174). This indicates that nanosized adsorbent of cedar leaf ash adsorbs cadmium ion more quickly and adsorption equilibrium time occurs rapidly, probably because of small size, large surface area, crystal shape, unique regular structure, and high reactivity of nanoparticles.

3.4. Effects of adsorbent amount

Fig. 9 shows the effect of the adsorbent amount on the adsorption percentage of cadmium. The trend shows that with the increasing adsorbent amount from 1 to 10 g L^{-1}, adsorption of cadmium increases extremely. After that, with increasing the adsorbent amount, the change of adsorption percentage is reduced slightly. Also the results indicate that for cadmium solution with initial concentration of 10 mg L^{-1}, the amount of 20 g L^{-1} nanoparticles of cedar leaf ash is sufficient and with increasing the amount of the adsorbent after this point, the adsorption percentage reduces.

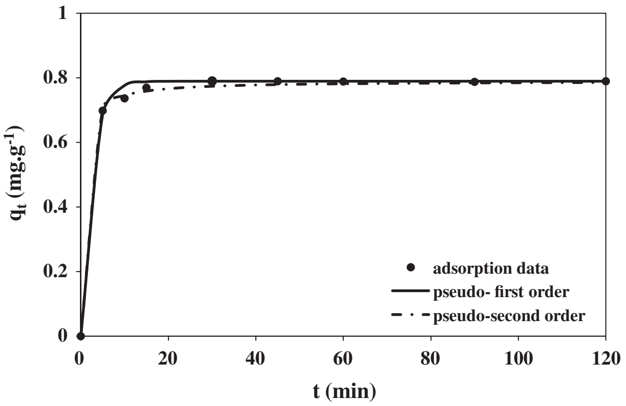

Fig. 7. Adsorption kinetics of cadmium ions on nanosized adsorbent of cedar leaf ash (initial concentration of solution, 10 mg L^{-1}; adsorbent amount, 10 g L^{-1}; pH 5).

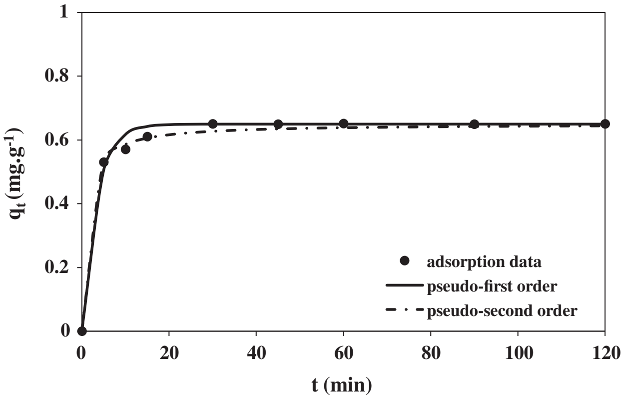

Fig. 8. Adsorption kinetics of cadmium ions on milli-sized adsorbent of cedar leaf ash (initial concentration of solution, 10 mg L^{-1}; adsorbent amount, 10 g L^{-1}; pH 5).

Considering the large surface area of nanoparticles, their reactivity is high and with increasing the adsorbent amount, nanoparticles aggregate and their surface area reduces and the adsorption efficiency of cadmium ions decreases. The results of other researchers confirm this [43]. On the other hand, with increasing the milli-sized adsorbent amount from 1 to

Table 4
Adsorption kinetic models parameters

Model	Parameter	Nanosized adsorbent	Milli-sized adsorbent
Pseudo-second-order	q_e	0.8	0.6640
	K_2	1.728	1.132
	R^2	0.9995	0.9981
	RMSE	0.00624	0.01223
Pseudo-first-order	q_e	0.782	0.6400
	K_1	0.4249	0.3174
	R^2	0.9969	0.9905
	RMSE	0.01531	0.02201

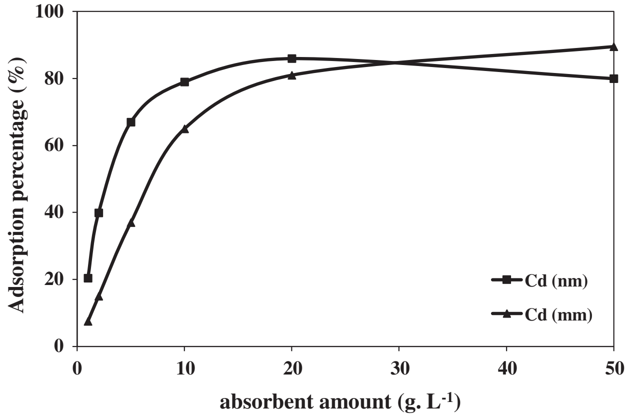

Fig. 9. Effect of adsorbent amount on adsorption of cadmium (initial concentration of solution, 10 mg L^{-1}; pH 5).

50 mg L^{-1}, the number of available adsorption sites increases and the trend of the adsorption efficiency of cadmium goes upward.

3.5. Isotherm studies

The isotherm parameters calculated from the Langmuir and Freundlich models are listed in Table 5, and the plots of two-mentioned models are shown in Figs. 10 and 11. For adsorption of cadmium by nanosized adsorbent of cedar leaf ash, the best fitting of experimental adsorption data was obtained by the Langmuir isotherm (RMSE = 0.06931 and $R^2 = 0.9957$) compared with Freundlich model (RMSE = 0.08916 and $R^2 = 0.9874$). Also this model has best fitting on cadmium adsorption data by milli-sized adsorbent of cedar leaf ash (RMSE = 0.1775 and $R^2 = 0.9733$).

The Freundlich isotherm exponent n values fulfilled the condition of $0 < n < 10$ for favorable adsorption [32]. This parameter for nano/milli-sized adsorbent of cedar leaf ash is 1.413 and 1.645, respectively.

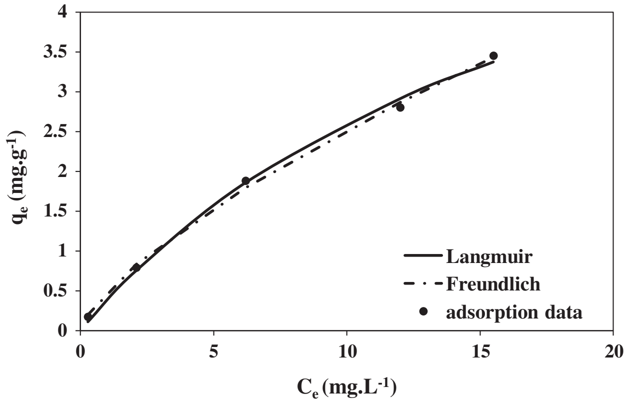

Fig. 10. Adsorption isotherm of cadmium ions on nanosized adsorbent of cedar leaf ash (adsorbent amount, 10 g L^{-1}; pH 5).

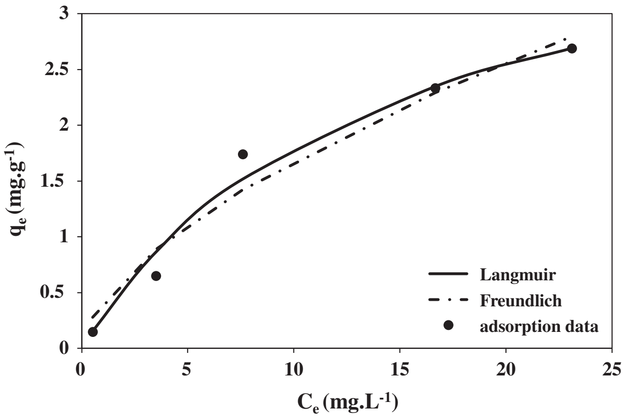

Fig. 11. Adsorption isotherm of cadmium ions on milli-sized adsorbent of cedar leaf ash (adsorbent amount, 10 g L^{-1}; pH 5).

Table 5
Adsorption isotherm models parameters

Model	Parameter	Nanosized adsorbent	Milli-sized adsorbent
Freundlich	n	1.413	1.645
	k	0.4933	0.4145
	R^2	0.9874	0.9467
	RMSE	0.08916	0.2507
Langmuir	b	0.0741	0.0714
	q_m	7.85	4.333
	R^2	0.9957	0.9733
	RMSE	0.06931	0.1775
	R_L	0.57	0.58

Comparison of the parameter q_m (Langmuir model) between the nano/milli-sized adsorbent of cedar leaf ash indicates that the maximum adsorption capacity of nanosized adsorbent (7.85 $\mathrm{mg\,g^{-1}}$) is almost two times higher than the milli-sized adsorbent (4.33 $\mathrm{mg\,g^{-1}}$). This case implies the ability of nanoparticles in adsorption of cadmium from aqueous solutions.

The essential characteristics of the Langmuir isotherm model can also be expressed in terms of a dimensionless constant of separation factor or equilibrium parameter, R_L, which is calculated using the following equation [32,44–48].

$$R_L = \frac{1}{(1 + b \times C_0)} \tag{4}$$

where b is the Langmuir constant, and C_0 is the initial concentration of metal ions.

R_L values between 0 and 1 indicate favorable adsorption, while $R_L > 1$, $R_L = 1$, and $R_L = 0$ indicate unfavorable, linear, and irreversible adsorption isotherms, respectively [32,47,48]. In this research, R_L for nano/milli-sized adsorbent of cedar leaf ash is 0.57 and 0.58, respectively which indicates the favorability adsorption of Langmuir model.

4. Conclusions

In this study, nano/milli-sized particles of cedar leaf ash were used as an adsorbent for the adsorption of cadmium from aqueous solutions. The adsorption process was evaluated by parameters such as pH, contact time, and adsorbent amount. The optimum solution of pH for the adsorption obtained was 5. The adsorption kinetic results showed that the adsorption of cadmium by both adsorbents mentioned followed the second-order kinetics model. The adsorption isotherm data were described well by the Langmuir isotherm model. The specific area of the nanosized particles is greater than that of the milli-sized particles, therefore the maximum adsorption capacity of the nanosized adsorbent was almost two times higher than the maximum adsorption capacity of milli-sized adsorbent (7.85 and 4.33 $\mathrm{mg\,g^{-1}}$). Furthermore, the findings indicate high capability of nanosized particles in adsorption of cadmium from aqueous solutions.

Acknowledgments

The authors would like to thank National Nanotechnology Initiative council of Iran and Shahid Chamran University of Ahwaz, Iran, for their financial and other supports.

References

[1] G. Zeng, Y. Pang, Z. Zeng, L. Tang, Y. Zhang, Y. Liu, J. Zhang, X. Lei, Z. Li, Y. Xiong, G. Xie, Removal and recovery of Zn^{2+} and Pb^{2+} by imine-functionalized magnetic nanoparticles with tunable selectivity, Langmuir 28 (1) (2012) 468–473.

[2] S. Govender, W. Zybylowicz, P. Swart, Removal of heavy metals from solution using biocompatible polymers, Desalin. Water Treat. 9 (2009) 272–278.

[3] Sh. Shamohamadi, M. Bustanian, H. Tavakol, Removing Cd^{2+} from water and wastewater by blowy sand; the effects of total hardness and pH, Desalin. Water Treat. 51 (2013) 3463–3471.

[4] M. Mhamdi, E. Elaloui, M. Trabelsi-Ayadi, Kinetics of cadmium adsorption by smectite of Oued Tfal (Gafsa Basin), Desalin. Water Treat. 52(22–24) (2014) 4245–4256.

[5] G. Yang, L. Tang, X. Lei, G. Zeng, Y. Cai, X. Wei, Y. Zhou, S. Li, Y. Fang, Y. Zhang, Cd(II) removal from aqueous solution by adsorption on ketoglutaric acid-modified magnetic chitosan, Appl. Surf. Sci. 292 (2014) 710–716.

[6] X.S. Wang, F. Liu, H.J. Lu, P. Zhang, H.Y. Zhou, Adsorption kinetics of Cd (II) from aqueous solution by magnetite, Desalin. Water Treat. 36 (2011) 203–209.

[7] S.M. Lee, C. Laldawngliana, D. Tiwari, Iron oxide nano-particles-immobilized-sand material in the treatment of Cu(II), Cd(II) and Pb(II) contaminated waste waters, Chem. Eng. J. 195–196 (2012) 103–111.

[8] R. Gong, W. Cai, N. Li, J. Chen, J. Liang, J. Cao, Preparation and application of thiol wheat straw as sorbent for removing mercury ion from aqueous solution, Desalin. Water Treat. 21 (2010) 274–279.

[9] K. Yogesh Kumar, H.P. Muralidhara, Y. Arthoba Nayaka, J. Balasubramanyam, Low-cost synthesis of mesoporous Zn(II)-Sn(II) mixed oxide nanoparticles for the adsorption of dye and heavy metal ion from aqueous solution, Desalin. Water Treat. (2013) 1–15.

[10] L. Tang, G.D. Yang, G.M. Zeng, Y. Cai, S.S. Li, Y.Y. Zhou, Y. Pang, Y.Y. Liu, Y. Zhang, B. Luna, Synergistic effect of iron doped ordered mesoporous carbon on adsorption-coupled reduction of hexavalent chromium and the relative mechanism study, Chem. Eng. J. 239 (2014) 114–122.

[11] Y.H. Wang, S.H. Lin, R.S. Juang, Removal of heavy metal ions from aqueous solutions using various low-cost adsorbents, J. Hazard. Mater. 102(2–3) (2003) 291–302.

[12] A. Rahmani, H. Gaffari, M.H. Saghi, M. Zarrabi, Application of nano matrials in water treatment, Fazaey. Nano. 18(4) (2008) 5–12.

[13] H. Aydin, Y. Bulut, C. Yerlikaya, Removal of copper (II) from aqueous solution by adsorption onto low-cost adsorbents, J. Environ. Manage. 87 (2008) 37–45.

[14] T.K. Naiya, P. Chowdhury, A.K. Bhattacharya, S.K. Das, Saw dust and neem bark as low-cost natural biosorbent for adsorptive removal of Zn(II) and Cd(II) ions from aqueous solutions, Chem. Eng. J. 148 (2009) 68–79.

[15] R. Ertas, N. Ozturk, Removal of lead from aqueous solutions by using chestnut shell as an adsorbent, Desalin. Water Treat. 51 (2013) 2903–2908.

[16] D. Sud, G. Mahajan, M.P. Kaur, Agricultural waste material as potential adsorbent for sequestering heavy metal ions from aqueous solutions—A review, Bioresour. Technol. 99 (2008) 6017–6027.

[17] A.H. Englert, J. Rubio, Characterization and environmental application of a Chilean natural zeolite, Int. J. Miner. Process. 75 (2005) 21–29.

[18] N. Yener, C. Biçer, M. Önal, Y. Sarıkaya, Simultaneous determination of cation exchange capacity and surface area of acid activated bentonite powders by methylene blue sorption, Appl. Surf. Sci. 258 (2012) 2534–2539.

[19] Y. Yukselen, A. Kaya, Suitability of the methylene blue test for surface area, cation exchange capacity and swell potential determination of clayey soils, Eng. Geol. 102 (2008) 38–45.

[20] D. Borah, K. Senapati, Adsorption of Cd(II) from aqueous solution onto pyrite, Fuel 85 (2006) 1929–1934.

[21] J.J.M. Órfão, A.I.M. Silva, J.C.V. Pereira, S.A. Barata, I.M. Fonseca, P.C.C. Faria, M.F.R. Pereira, Adsorption of a reactive dye on chemically modified activated carbons-influence of pH, J. Colloid Interface Sci. 296 (2006) 480–489.

[22] N. Najafi, Y. Yousefi, A.A. Rafati, Synthesis, characterization and adsorption studies of several heavy metal ions on amino-functionalized silica nano hollow sphere and silica gel, Sep. Purif. Technol. 85 (2012) 193–205.

[23] Y. Niu, R. Qu, C. Sun, C. Wang, H. Chen, C. Ji, Y. Zhang, X. Shao, F. Bu, Adsorption of Pb(II) from aqueous solution by silica-gel supported hyperbranched polyamidoamine dendrimers, J. Hazard. Mater. 244–245 (2013) 276–286.

[24] H. Chen, J. Zhao, G. Dai, J. Wu, H. Yan, Adsorption characteristics of Pb(II) from aqueous solution onto a natural biosorbent, fallen *Cinnamomum camphora* leaves, Desalination 262 (2010) 174–182.

[25] T. Wang, W. Liu, N. Xu, J. Ni, Adsorption and desorption of Cd(II) onto titanate nanotubes and efficient regeneration of tubular structures, J. Hazard. Mater. 250–251 (2013) 379–386.

[26] J. Sirajudeen, J. Naveen, S. Arul Manikandan, M.M. Mohamed Mubashir, Removal of chromium (VI) from aqueous solution by using *Citrus limetta* Peel as an adsorbent, Der. Chem. Sin. 4(2) (2013) 133–143.

[27] H.K. Boparai, M. Joseph, D. O'Carroll, Kinetics and thermodynamics of cadmium ion removal by adsorption onto nano zerovalent iron particles, J. Hazard. Mater. 186 (2011) 458–465.

[28] R. Malekian, J. Abedi-Koupai, S.S. Eslamian, S.F. Mousavi, K.S. Abbaspour, M. Afyuni, Ion-exchange process for ammonium removal and release using natural Iranian zeolite, Appl. Clay. Sci. 51 (2011) 323–329.

[29] J. Fabrianto, A. Natasia Kosasiah, J. Sunarso, Y.H. Ju, Equilibrium and kinetic studies in adsorption of heavy metals using biosorbent: A summary of recent studies, J. Hazard. Mater. 162 (2009) 616–645.

[30] I. Langmuir, The adsorption of gases on plane surfaces of glass, mica and platinum, J. Am. Chem. Soc. 40 (1918) 1361–1403.

[31] H. Ebrahimian, A. Liaghat, Field evaluation of various mathematical models for furrow and border irrigation systems, Soil. Water Res. 6(2) (2011) 91–101.

[32] A. Afkhami, M. Saber-Tehrani, H. Bagheri, Simultaneous removal of heavy-metal ions in wastewater samples using nano-alumina modified with 2, 4-dinitrophenylhydrazine, J. Hazard. Mater. 181 (2010) 836–844.

[33] Z. Li, X. Tang, Y. Chen, L. Wei, Y. Wang, Batch activation of firmiana simplex leaf and the enhanced Pb(II) adsorption performance: Equilibrium and kinetic studies, J. Hazard. Mater. 169 (2009) 386–394.

[34] J.H. Chen, H.T. Xing, H.X. Guo, G.P. Li, W. Weng, S.R. Hu, Preparation, characterization and adsorption properties of a novel 3-aminopropyltriethoxysilane functionalized sodium alginate porous membrane adsorbent for Cr(III) ions, J. Hazard. Mater. 248–249 (2013) 285–294.

[35] S. Shrestha, G. Son, S.H. Lee, T.G. Lee, Isotherm and thermodynamic studies of Zn (II) adsorption on lignite and coconut shell-based activated carbon fiber, Chemosphere 92 (2013) 1053–1061.

[36] S. Qaiser, A.R. Saleemi, M. Umar, Biosorption of lead from aqueous solution by ficus religiosa leaves: Batch and column study, J. Hazard. Mater. 166 (2009) 998–1005.

[37] W.S. Wan Ngah, M.A.K.M. Hanafiah, Biosorption of copper ions from dilute aqueous solutions on base treated rubber (*Hevea brasiliensis*) leaves powder: Kinetics, isotherm, and adsorption mechanisms, J. Environ. Sci. 20 (2008) 1168–1176.

[38] A. Mahapatra, B.G. Mishra, G. Hota, Electrospun Fe_2O_3–Al_2O_3 nanocomposite fibers as efficient adsorbent for removal of heavy metal ions from aqueous solution, J. Hazard. Mater. 258–259 (2013) 116–123.

[39] S.H. Huang, D.H. Chen, Rapid removal of heavy metal cations and anions from aqueous solutions by an amino-functionalized magnetic nano-adsorbent, J. Hazard. Mater. 163(1) (2009) 174–179.

[40] F. Mohammed-Azizi, S. Dib, M. Boufatit, Removal of heavy metals from aqueous solutions by Algerian bentonite, Desalin. Water Treat. 51 (2013) 4447–4458.

[41] D. Zhang, C.L. Zhang, P. Zhou, Preparation of porous nano-calcium titanate microspheres and its adsorption behavior for heavy metal ion in water, J. Hazard. Mater. 186 (2011) 971–977.

[42] S. Bayar, A.E. Yilmaz, R. Boncukcuoglu, B.A. Fil, M.M. Kocakerim, Effects of operational parameters on cadmium removal from aqueous solutions by electrochemical coagulation, Desalin. Water Treat. 51 (2013) 2635–2643.

[43] A. Rahmani, H. Zavvar Mousavi, M. Fazli, Effect of nanostructure alumina on adsorption of heavy metals, Desalination 253(1–3) (2010) 94–100.

[44] E. Demirbas, M.Z. Nas, Batch kinetic and equilibrium studies of adsorption of Reactive Blue 21 by fly ash and sepiolite, Desalination 243 (2009) 8–21.

[45] M. Xu, Y. Zhang, Z. Zhang, Y. Shen, M. Zhao, G. Pan, Study on the adsorption of Ca^{2+}, Cd^{2+} and Pb^{2+} by magnetic Fe_3O_4 yeast treated with EDTA dianhydride, Chem. Eng. J. 168 (2011) 737–745.

[46] C. Theivarasu, S. Mylsamy, Equilibrium and kinetic adsorption studies of rhodamine-B from aqueous solutions using cocoa (*Theobroma cacao*) shell as a new adsorbent, Int. J. Eng. Sci. Technol. 2(11) (2010) 6284–6292.

[47] Y. Zhao, Y. Xia, H. Yang, Y. Wang, M. Zhao, Synthesis of glutamic acid-modified magnetic corn straw: Equilibrium and kinetic studies on methylene blue adsorption, Desalin. Water Treat. (2013) 1–9.

[48] P. Lim, A.Z. Aris, A novel approach for the adsorption of cadmium ions in aqueous solution by dead calcareous skeletons, Desalin. Water Treat. (2013) 1–9.